Directionality in Cardiovascular Variability Interactions during Head-Down Tilt Test

Alberto Porta, *IEEE Member*, Andrea Marchi, Vlasta Bari, Aparecida M. Catai, Stefano Guzzetti, Ferdinando Raimondi, and Riccardo Colombo

***Abstract*— A nonlinear model-free Granger causality approach was exploited to quantify the strength of the causal relation along cardiac baroreflex and cardiopulmonary pathway from spontaneous cardiovascular variabilities during head-down tilt (HDT). The analysis was completed through the assessment of traditional time and frequency domain parameters and cardiac baroreflex sensitivity. We found that, while respiratory sinus arrhythmia augmented, the power of the systolic arterial pressure variability in the low frequency band (i.e. from 0.04 to 0.15 Hz) decreased and cardiac baroreflex sensitivity increased, the strength of the causal relation along cardiac baroreflex and cardiopulmonary pathway remained constant. We conclude that, despite cardiopulmonary stimulation and sympathetic inhibition induced by HDT, neither cardiac baroreflex nor cardiopulmonary pathway took prevalence in governing heart period changes during HDT.**

I. Introduction

Head-up tilt unloads baroreflex by reducing venous return and central venous pressure, thus leading to a reflex sympathetic activation [1,2]. When the dynamical interactions among heart period (HP), systolic arterial pressure (SAP) and respiratory activity (RESP) variability were assessed during head-up tilt, it was found that cardiac baroreflex sensitivity (BRS) decreased [2], the strength of the causal relation along cardiac baroreflex (i.e. from SAP to HP) augmented [3,4] and the coupling along cardiopulmonary pathway (i.e. from RESP to HP) decreased [4] as a likely consequence of the sympathetic activation, solicitation of cardiac baroreflex and vagal withdrawal respectively.

Head-down tilt (HDT) loads baroreflex by increasing venous return and central venous pressure and stimulate cardiopulmonary pathway [5], thus leading to a sympathetic inhibition [6]. While it is well-established that BRS was improved during HDT [7,8], the effects over the strength of the causal relation along cardiac baroreflex and cardiopulmonary pathway are unknown. Since the HDT is a relevant stimulus for the cardiopulmonary pathway, we hypothesize that the magnitude of the coupling from RESP to HP increases, while the strength of the causal relation from SAP to HP loses importance.

The aim of the study is to assess the dynamical interactions from SAP to HP, along the cardiac baroreflex, and from RESP to HP, along the cardiopulmonary pathway, via a recently proposed Granger causality approach [9] during HDT. The analysis was supplemented by the calculation of more traditional time and frequency domain parameters [10,11].

II. Nonlinear Model-Free Granger Causality Approach

We exploited the original definition of Granger causality [12] stating that, given an universe of knowledge $\Omega=\{X,Y,Z\}$ with $X=\{x(i),\ i,\ldots,N\}$, $Y=\{y(i),\ i,\ldots,N\}$ and $Z=\{z(i),\ i,\ldots,N\}$, where i is the progressive sample counter and N is the series length, X Granger-causes Y in Ω if the current value of Y, y(i), can be predicted better using past values of all the series in Ω than using past values of the series in Ω after excluding the presumed cause, X (i.e. $\Omega\backslash X=\{Y,Z\}$).

The presence of a causal link from X to Y was tested through the approach proposed in [9]. This strategy is based on the concept of local predictability [13]. It relies on the construction of a multivariate embedding space via the delay embedding procedure and on the assessment of the degree of unpredictability of the assigned effect series, Y, in Ω via the k-nearest-neighbor approach. The adopted approach is model-free because it does not make any specific assumption on the dynamical relationship among the series in Ω [13]. Briefly, the multivariate embedding space was built incrementally starting from a set of initial candidate samples, $\{x(i-\tau_X^Y),\ldots,x(i-\tau_X^Y-p),y(i-1),\ldots,y(i-p),z(i-\tau_Z^Y),\ldots,z(i-\tau_Z^Y-p)\}$ where τ_X^Y and τ_Z^Y are the delays from X and Z to Y and p is the maximal number of components for each signal. The procedure selected the delayed sample in the set of candidates that minimized the uncorrelation between the original and predicted values of Y. This sample was retained and the procedure of selection restarted again after discarding from the set of candidates the selected sample and all values more recent than it. This process led to the construction of a non uniform multivariate embedding space because samples might be oddly spaced in time and might belong to different signals. The procedure for the construction of the multivariate embedding space was stopped when the multivariate embedding dimension, q^Y,

A. Porta is with Department of Biomedical Sciences for Health, IRCCS Galeazzi Orthopedic Institute, University of Milan, Milan, Italy (tel: +39 02 50319976; fax: +39 02 50319979; email: alberto.porta@unimi.it).

A. Marchi and V. Bari are with Department of Electronics Information and Bioengineering, Politecnico di Milano, Milan, Italy (emails: andrea.marchi@polimi.it and vlasta.bari@polimi.it).

A.M. Catai is with Department of Physiotherapy, Federal University of São Carlos, São Carlos, Brazil (email: mcatai@ufscar.br).

S. Guzzetti and R. Colombo are with Department of Emergency, "L. Sacco" Hospital, Milan, Italy (emails: guzzetti.stefano@hsacco.it and colombo.riccardo@hsacco.it).

F. Raimondi is with Department of Anesthesia and Intensive Care, IRCCS Humanitas Clinical and Research Center, Rozzano, Italy (email: ferdinando.raimondi@humanitas.it).

978-1-4244-7929-0/14/$26.00 ©2014 IEEE

was equal to 15. The global minimum of the uncorrelation between the original and predicted Y series over q^Y was taken as a measure of the unpredictability of Y in Ω and the embedding dimension at the minimum, q_o^Y, was the one providing the best description of the causal interactions from X to Y in Ω (i.e. the optimal multivariate embedding dimension). The quantification of the magnitude of the causal relation from X to Y in Ω was performed via the computation of the causality ratio (CR). CR assessed the fractional decrease of the uncorrelation between original and predicted Y series resulting from the introduction of X in Ω\X [9]. Negative CR values indicated X brought valuable information about the future evolution of Y that could not be derived from any signal in Ω\X and, according to the concept of Granger causality [12], we stated that X Granger-caused Y in Ω.

III. Experimental Protocol and Data Analysis

A. Experimental Protocol

We studied 14 healthy men aged from 41 to 71 years (median: 59 years). A detailed medical history and examination excluded the evidence of any disease. The subjects did not take any medication, nor did they consume any caffeine or alcohol containing beverages in the 24h before the recording. The study adhered to the principles of the Declaration of Helsinki for medical research involving human subjects. The human research and ethical review board of the "L. Sacco" Hospital approved the protocol. All patients gave their written informed consent. Electrocardiogram (ECG) and noninvasive finger blood pressure (Nexfin, BMEYE, Amsterdam, The Netherlands) were recorded during the experiments. Signals were sampled at 400 Hz. Each experiment consisted of 10 minutes of baseline recording at rest in supine position (REST) followed by 10 minutes of recording during HDT with the table inclination of -25 degrees. Before REST we allowed 15 minutes of stabilization. During the protocol, the subjects breathed following a metronome at 16 breaths·minute^{-1} and they were not allowed to talk.

B. Beat-to-beat Series Extraction

After detecting the QRS complex on the ECG and locating the QRS peak using parabolic interpolation, the temporal distance between two consecutive QRS apexes was computed and utilized as an approximation of HP. The maximum of arterial pressure inside the i-th HP (i.e. HP(i)) was taken as the i-th SAP (i.e. SAP(i)). RESP was obtained from the respiratory-related amplitude modulation of the ECG. The amplitude of the first QRS complex delimiting HP(i) was taken as the i-th RESP (i.e. RESP(i)). The occurrences of QRS and SAP peaks were carefully checked to avoid erroneous detections or missed beats. If isolated ectopic beats affected HP and SAP values, these measures were linearly interpolated using the closest values unaffected by ectopic beats. HP, SAP and RESP measures were performed on a beat-to-beat basis. Sequences of 300 values were randomly selected inside each experimental condition. The series were linearly detrended. If evident nonstationarities, such as very slow drifting of the mean or sudden changes of the variance, were visible despite the linear detrending, the random selection was carried out again. The HP and SAP mean and the HP and SAP variance were indicated as μ_{HP}, μ_{SAP}, σ^2_{HP} and σ^2_{SAP} and expressed in ms, mmHg, ms^2 and mmHg^2 respectively.

C. Spectral Analysis

Power spectrum was estimated according to a parametric approach fitting the series with an autoregressive model [14]. Autoregressive spectral density was factorized into components each of them characterized by a central frequency. A spectral component was labeled as low frequency (LF) if its central frequency was between 0.04 and 0.15 Hz, while it was classified as high frequency (HF) if its central frequency was between 0.15 and 0.5 Hz [10]. The LF and HF powers were defined as the sum of the powers of all LF and HF spectral components respectively. The HF power of HP series, HF_{HP}, expressed in absolute units (ms^2), was utilized as an estimate of the respiratory sinus arrhythmia and a marker of vagal modulation directed to the sinus node [15], while the LF power of SAP series, LF_{SAP}, expressed in absolute units (mmHg^2), was utilized as a marker of sympathetic modulation directed to vessels [14].

D. BRS Estimate

We assessed BRS according to the spectral method [11]. We computed the square root of the ratio of the power of HP on that of SAP in the LF and HF bands as BRS indexes (α_{LF} and α_{HF} respectively). α_{LF} and α_{HF} were expressed in ms·mmHg^{-1}. The reliability of α_{LF} and α_{HF} was tested by checking at the frequency of interest that HP and SAP series were significantly associated and HP changes lagged behind SAP variations [16]. These prerequisites were tested according to the calculation of squared coherence function ($K^2_{HP,SAP}$) and phase spectrum ($Ph_{HP\text{-}SAP}$). $K^2_{HP,SAP}$ was computed as the ratio of the square HP-SAP cross-spectrum modulus divided by the product of the power spectra of HP and SAP series. $K^2_{HP,SAP}$ ranged between 0 and 1 indicating null and perfect association between HP and SAP series, respectively. As suggested in [16], $K^2_{HP,SAP}>0.5$ was taken as an indication of the presence of a significant HP-SAP correlation. $Ph_{HP\text{-}SAP}$ was the phase of the HP-SAP cross-spectrum. It was expressed in radians and ranged between $+\pi$ and $-\pi$ indicating phase opposition. With the convention adopted for the computation of the HP-SAP cross-spectrum $Ph_{HP\text{-}SAP}<0.0$ suggested that HP changes lagged behind SAP variations. The HP-SAP cross-spectrum was estimated according to a bivariate parametric approach [17]. $K^2_{HP,SAP}$ and $Ph_{HP\text{-}SAP}$ were sampled in correspondence of the weighted average of the central frequencies detected on the SAP series in the LF and HF bands, where the weights were the powers of the components. These values were labeled as $K^2_{HP,SAP}(LF)$, $Ph_{HP\text{-}SAP}(LF)$, $K^2_{HP,SAP}(HF)$ and $Ph_{HP\text{-}SAP}(HF)$ in the following.

E. Calculation of CR Indexes

We considered an universe of knowledge, Ω, formed by {HP, SAP, RESP} for the calculation of CR indexes. After normalizing each series to have zero mean and unit variance, we calculated CR from SAP to HP in Ω, as a measure of the

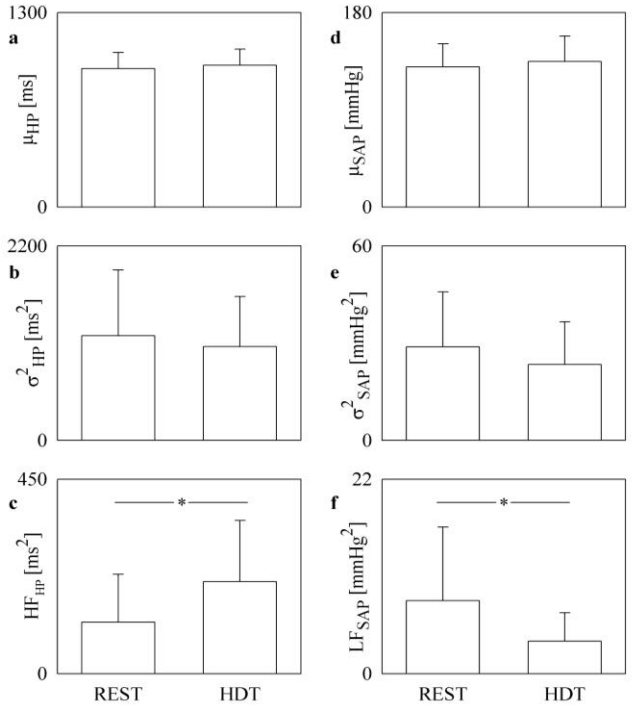

Fig.1. Bar graphs show μ_{HP} (a), σ^2_{HP} (b), HF_{HP} (c), μ_{SAP} (d), σ^2_{SAP} (e), LF_{SAP} (f) at REST and during HDT. Values are reported as mean+standard deviation. The symbol * indicates a significant difference with $p<0.05$.

strength of the causal link along cardiac baroreflex, $CR_{SAP\rightarrow HP}$, and CR from RESP to HP in Ω, $CR_{RESP\rightarrow HP}$, as a measure of the strength of the causal link along cardiopulmonary pathway. The parameter p and q^Y were set to 10 and 15 respectively. The delay from SAP to HP, $\tau_{SAP}{}^{HP}$, and from RESP to HP, $\tau_{RESP}{}^{HP}$, was set to 0, thus allowing the description of the fast vagal arm of cardiac baroreflex and cardiopulmonary pathway [17]. The best multivariate embedding space in $\Omega\backslash X$ with X=SAP or RESP was obtained from the best multivariate embedding space in Ω by discarding components relevant X for the calculation of $CR_{X\rightarrow HP}$. The number of nearest neighbors was set to 30.

F. Statistical Analysis

We performed paired t-test to check the significance of the difference between indexes at REST and during HDT. If the normality test (Kolmogorov-Smirnov test) was not fulfilled, Wilcoxon signed rank test was utilized. Since it occurred that the prerequisites for the computation of BRS were not fulfilled in both experimental conditions, unpaired t-test was utilized to test the significance of the difference between BRS indexes at REST and during HDT. If the normality test was not passed, Mann-Whitney rank sum test was exploited. χ^2 test (McNemar's test) was exploited to check whether HDT affected the percentage of subjects with CR smaller than 0. Statistical analysis was carried out using a commercial statistical program (SigmaPlot 11.0, Systat Software Inc., San Jose, CA, USA). A $p<0.05$ was always considered as significant.

IV. RESULTS

Figure 1 shows time and frequency domain indexes as a function of the experimental condition (i.e. REST and HDT). Time domain indexes were not affected by HDT: indeed, μ_{HP}, σ^2_{HP}, μ_{SAP} and σ^2_{SAP} were similar to those computed at REST. Conversely, frequency domain parameters were influenced by HDT: indeed, while HF_{HP} significantly increased, LF_{SAP} significantly decreased.

Figure 2 shows α_{LF} (Fig.2a) and α_{HF} (Fig.2b) at REST and during HDT. Values are computed over those subjects with $K^2_{HP,SAP}(LF)>0.5$ and $Ph_{HP\text{-}SAP}(LF)<0.0$ in the case of Fig.2a and with $K^2_{HP,SAP}(HF)>0.5$ and $Ph_{HP\text{-}SAP}(HF)<0.0$ in the case of Fig.2b. The percentage of subjects with $K^2_{HP,SAP}(LF)>0.5$ and $Ph_{HP\text{-}SAP}(LF)<0.0$ were 86% at REST and 79% during HDT, while those with $K^2_{HP,SAP}(HF)>0.5$ and $Ph_{HP\text{-}SAP}(HF)<0.0$ were smaller (i.e. 50% at REST and 64% during HDT). Both α_{LF} and α_{HF} were larger during HDT, but only α_{HF} was significantly increased (Fig.2b).

The optimal embedding dimension, q_o^{HP}, ranged between 2 and 6 both at REST and during HDT. Since q_o^{HP} was largely below the settings imposed to p and q^{HP} (i.e. p=10 and q^{HP}=15), we concluded that the proposed settings were adequate to explore the casual interactions from SAP and RESP to HP. Granger causality analysis suggested that $CR_{SAP\rightarrow HP}$ was smaller than 0, thus indicating a significant HP-SAP link along baroreflex, in 57% of the subjects, and $CR_{RESP\rightarrow HP}$ was smaller than 0, thus indicating a significant HP-RESP link along cardiopulmonary pathway, in 71% of the subjects. $CR_{SAP\rightarrow HP}$ and $CR_{RESP\rightarrow HP}$ were 0 in the remaining subjects. HDT did not significantly modify these percentages. Similarly to the percentage of subjects with significant causal link, $CR_{SAP\rightarrow HP}$ and $CR_{RESP\rightarrow HP}$ were not influenced by HDT as well (Fig.3).

V. DISCUSSION

HDT is an experimental condition increasing venous return and central venous pressure, thus stimulating low pressure receptors in the atrium and cardiopulmonary baroreflex. Since cardiopulmonary baroreflex inhibits sympathetic activity [5,6], it is not surprising to find out that, during HDT, the power of HP variability in the HF band, i.e. a marker of vagal modulation directed to the sinus node [15], increased, the power of the SAP variability in the LF band, i.e. a marker of sympathetic modulation directed to vessels [14], decreased, and BRS, estimated according to the spectral method [11], improved [7]. The present study confirmed all these findings as well as the inability of HDT to affect HP and SAP means [5].

While traditional signal processing tools, such as spectral and cross-spectral analyses, have been frequently applied to HP and SAP variabilities during HDT to infer the state of the

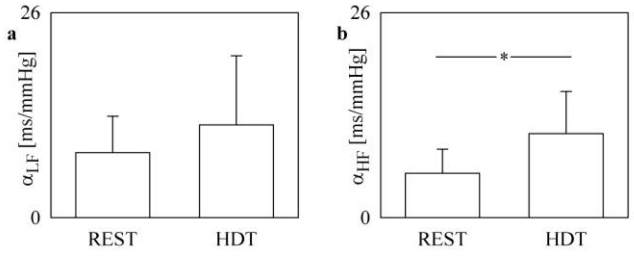

Fig.2. Bar graphs shows α_{LF} and α_{HF} assessed via spectral technique from HP and SAP series at REST and during HDT. Values are reported as mean+standard deviation. The symbol * indicates a significant difference with $p<0.05$.

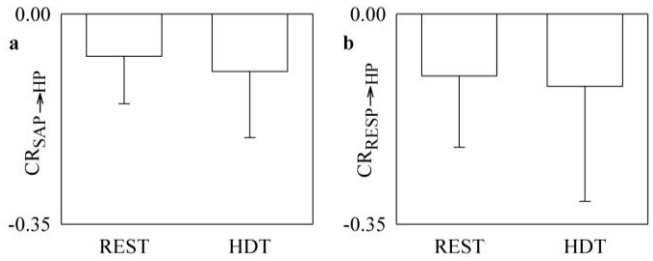

Fig.3. Bar graphs shows CR from SAP to HP, $CR_{SAP \rightarrow HP}$ (a), and CR from RESP to HP, $CR_{RESP \rightarrow HP}$ (b) at REST and during HDT. Values are reported as mean-standard deviation.

autonomic nervous system, no information were provided about the degree of association among cardiovascular variabilities especially in a given temporal direction (e.g. from SAP to HP along cardiac baroreflex and from RESP to HP along cardiopulmonary pathway). Causality analysis provides an unique opportunity to assess the degree of association between two series in a given temporal direction (i.e. from a presumed cause signal to the assigned effect one) in terms of unpredictability decrement of the effect signal that can be attributed solely to the introduction of the cause signal in the restricted description of the dynamical behavior of the system (i.e. Ω after excluding the cause signal). When causality analysis was applied to head-up tilt, i.e. an experiment condition providing the opposite effect on central venous pressure and venous return compared to HDT, we found an increased strength of the causal relation along cardiac baroreflex (i.e. from SAP to HP) and a decreased magnitude of the cardiopulmonary coupling (i.e. from RESP to HP) [3,4]. These findings were interpreted as the consequence of the important baroreflex solicitation and of the vagal withdrawal observed during head-up tilt. Since HDT stimulates cardiopulmonary pathway and limits the importance of cardiac baroreflex in governing HP-SAP variability interactions, the opposite result is expected (i.e. an increased strength of the causal relation from RESP to HP and a decreased magnitude of the causal relation from SAP to HP). Contrary to our expectations the strength of the causal coupling from SAP and RESP to HP was unchanged. We attribute this unexpected result to the contemporaneous action of both cardiac baroreflex and cardiopulmonary pathway, neither taking preeminence over the other in governing HP variability and both contributing to maintain high the complexity of the cardiac control.

VI. Conclusion

Causality analysis complemented more traditional tools in time and frequency domains and provided a framework to assess the dynamical interactions among spontaneous cardiovascular variabilities. This analysis suggested that during HDT cardiopulmonary pathway did not take a preeminent role over cardiac baroreflex in regulating HP changes and both reflexes contributed to the HP complexity.

The large scatter of age in our group could be a possible limitation of the present study. Therefore, we advocate studies focusing narrower age ranges and checking the possible dependence of the findings on age. In addition, future studies should directly measure central venous pressure and obtain RESP series from it instead of using the respiratory modulation of the ECG as a surrogate measure of respiratory oscillations of central venous pressure.

References

[1] R. Furlan, A. Porta, F. Costa, J. Tank, L. Baker, R. Schiavi, D. Robertson, A. Malliani, and R. Mosqueda-Garcia, "Oscillatory patterns in sympathetic neural discharge and cardiovascular variables during orthostatic stimulus," *Circulation* vol. 101, pp. 886-892, 2000.

[2] W.H. Cooke, J.B. Hoag, A.A. Crossman, T.A. Kuusela, K.U.O. Tahvanainen, and D.L. Eckberg, "Human responses to upright tilt: a window on central autonomic integration," *J. Physiol.* vol. 517, pp. 617-628, 1999.

[3] A. Porta, A.M. Catai, A.C.M. Takahashi, V. Magagnin, T. Bassani, E. Tobaldini, P. van de Borne, and N. Montano, "Causal relationships between heart period and systolic arterial pressure during graded head-up tilt," *Am. J. Physiol.* vol. 300, pp. R378-R386, 2011.

[4] A. Porta, T. Bassani, V. Bari, E. Tobaldini, A.C.M. Takahashi, A.M. Catai, and N. Montano, "Model-based assessment of baroreflex and cardiopulmonary couplings during graded head-up tilt," *Comput. Biol. Med.* vol. 42, pp. 298-305, 2012.

[5] H. Tanaka, K.P. Davy, and D.R. Seals, "Cardiopulmonary baroreflex inhibition of sympathetic nerve activity is preserved with age in healthy humans," *J. Physiol.* vol. 515, pp. 249-254, 1999.

[6] K. Nagaya, P. Wada, S. Nakamitsu, S. Sagawa, and K. Shiraki, "Responses of the circulatory system and muscle sympathetic nerve activity to head-down tilt in humans," *Am. J. Physiol.* vol. 268, R1289-R1294, 1995.

[7] A. Kardos, L. Rudas, J. Simon, Z. Gingl, and M. Csanady, "Effect of postural changes on arterial baroreflex sensitivity assessed by the spontaneous method and Valsalva manoeuvre in healthy subjects," *Clin. Auton. Res.* vol. 7, pp. 143-148, 1997.

[8] M.H. Harrison, D. Rittenhouse, and J.E: Greenleaf, "Effect of posture on arterial baroreflex control of heart rate in humans," *Eur. J. Appl. Physiol.* vol. 55, pp. 367-373, 1986.

[9] A. Porta, L. Faes, V. Bari, A. Marchi, T. Bassani, G. Nollo, N.M. Perseguini, J. Milan, V. Minatel, A. Borghi-Silva, A.C.M. Takahashi, and A.M. Catai, "Effect of age on complexity and causality of the cardiovascular control: comparison between model-based and model-free approaches," *PLoS ONE* vol. 9, e89463, 2014.

[10] Task Force of the European Society of Cardiology and the North American Society of Pacing and Electrophysiology, "Standard of measurement, physiological interpretation and clinical use," *Circulation* vol. 93, pp. 1043-1065, 1996.

[11] M. Pagani, V.K. Somers, R. Furlan, S. Dell'Orto, J. Conway, G. Baselli, S. Cerutti, P. Sleight, and A. Malliani, "Changes in autonomic regulation induced by physical training in mild hypertension," *Hypertension* vol. 12, pp. 600-610, 1988.

[12] C.W.J. Granger, "Testing for causality. A personal viewpoint," *J. Econ. Dyn. Control.* vol. 2, pp. 329-352, 1980.

[13] H.D.I. Abarbanel, T.L. Carroll, L.M. Pecora, J.J. Sidorowich, and L.S. Tsimring, "Predicting physical variables in time-delay embedding," *Phys. Rev. E* vol. 49, pp. 1840-1853, 1994.

[14] M. Pagani, F. Lombardi, S. Guzzetti, O. Rimoldi, R. Furlan, P. Pizzinelli, G. Sandrone, G. Malfatto, S. Dell'Orto, E. Piccaluga, M. Turiel, G. Baselli, S. Cerutti, and A. Malliani, "Power spectral analysis of heart rate and arterial pressure variabilities as a marker of sympatho-vagal interaction in man and conscious dog," *Circ. Res.* vol. 59, pp. 178-193, 1986.

[15] S. Akselrod, D. Gordon, F.A. Ubel, D.C. Shannon, R.D. Berger, and R.J. Cohen, "Power spectrum analysis of heart rate fluctuations: a quantitative probe of beat-to-beat cardiovascular control," *Science* vol. 213, pp. 220-223, 1981.

[16] R.W. De Boer, J.M. Karemaker, and J. Strackee, "Relationships between short-term blood pressure fluctuations and heart rate variability in resting subjects I: a spectral analysis approach," *Med. Biol. Eng. Comput.* vol. 23, pp. 352-358, 1985.

[17] A. Porta, G. Baselli, O. Rimoldi, A. Malliani, and M. Pagani, "Assessing baroreflex gain from spontaneous variability in conscious dogs: role of causality and respiration," *Am. J. Physiol.* vol. 279, pp. H2558-H2567, 2000.